M. Dima
F.B.-8 Physik, Universität Wuppertal,
Gaußstr. 20, Wuppertal D-42097,
GERMANY

Generalising the methods used in the analysis of ATLAS Pixel Detectors test-beam data, line and helix fit flash-algorithms based on semi/analytical methods are presented. Routines based on this approach are over 3000 times faster than the traditional iterative procedures, yielding a 60 fold increase in alignment resolution for the same amount of CPU time.

I. INTRODUCTION

The present Note is intended for track-reconstruction, detector-alignment and detector-evaluation groups.

Often regarded as a simple problem, track reconstruction can soon become tangled with prohibitive CPU load and unexpectedly large errors. Detector alignment for instance requires that alignment parameters satisfy proper track reconstruction in all events. Tunning however the alignment parameters reconstructing all tracks in all events for each iteration[1] in parameter space is CPU exhausting, and in practice can be applied only to blocks of *i.e.* - 2000 tracks. If the track fits are also iterative, double-nesting[2] occurs and CPU times reach on the order of 2-4 days for line-fits respectively 20-300 days for helix-fits, in the context of the ATLAS Pixel Detector test-stand. On the other hand if the track fits are semi/analytical, CPU times are 3-4 orders of magnitude smaller and such an approach becomes feasable.

The note starts with the basic χ^2 fit, examines the validity of the standard χ^2 approximation in reconstruction contexts specific to ATLAS Pixel Detectors, gives analytical and semi-analytical track reconstruction solutions and presents examples of CPU-clocked processes on a DEC ALPHA machine[3].

[1]The majority of detectors are aligned iteratively, however an example of an analytical alignment method - for the (SLAC) SLD End-Cap Čerenkov Ring Imaging Detector, is described in [1].

[2]In fact triple-nesting since the determination of track-parameters and position on-track of the fitted points already is double-nesting.

[3]DEC-ALPHA 878 machine, EV 5.6 processor at 433 MHz, 640 MB RAM, running under OSF1 V4.0.

II. GENERAL FITS

The general χ^2 expression for a fit is the sum of normalised-residuals for a set of experimental points running from $j = \overline{1, N}$:

$$\chi^2 \stackrel{\text{def}}{=} \sum_{j=1}^{N} \frac{\Delta_j^2}{\sigma^2_{j_{(\Delta)}}} \tag{1}$$

where the error of the j^{th}-residual $\sigma_{j_{(\Delta)}}$ is related to the direction $|\Delta_j\rangle$ into which this residual is pointing:

$$\sigma^2_{j_{(\Delta)}} = \frac{\langle\Delta_j|\sigma_j^2|\Delta_j\rangle}{\langle\Delta_j|\Delta_j\rangle} \tag{2}$$

$\langle A|B\rangle$ denoting here scalar product. This leads to a χ^2 expression:

$$\chi^2_{exact} = \sum_{j=1}^{N} \frac{\langle\Delta_j|\Delta_j\rangle^2}{\langle\Delta_j|\sigma_j^2|\Delta_j\rangle} \tag{3}$$

More often however, a quadratic[4] approximation of χ^2_{exact} is used:

$$\chi^2_{approx} \stackrel{\text{def}}{=} \sum_{j=1}^{N} \langle\Delta_j|\sigma_j^{-2}|\Delta_j\rangle \tag{4}$$

with the equivalent residual error:

$$\sigma^2_{j_{(\Delta)}} = \frac{\langle\Delta_j|\Delta_j\rangle}{\langle\Delta_j|\sigma_j^{-2}|\Delta_j\rangle} \tag{5}$$

If a track impacts the error ellipsoids at an angle n = tg(θ_{incid}) with respect to one of the principal axes, under the assumption of $|\Delta_j\rangle$ approximately perpendicular to the trajectory, the two σ's are:

$$\sigma^2_{exact} \simeq \frac{\sigma^2_{xy} + n^2\sigma^2_z}{1+n^2}$$

$$\sigma^2_{approx} \simeq \frac{1+n^2}{\sigma^{-2}_{xy} + n^2\sigma^{-2}_z} \tag{6}$$

[4]$\langle\Delta_j|\sigma_j^{-2}|\Delta_j\rangle = \Delta_x^2/\sigma_x^2 + \Delta_y^2/\sigma_y^2 + \Delta_z^2/\sigma_z^2$.

both reducing to σ_{xy}^2 or σ_z^2 for tracks impacting along one of the principal axes.

The Telescope test-stand used to evaluate the ATLAS Inner Detector Pixel Modules is composed of 4 Sirocco Detectors as tracking elements and 1 or 2 Pixel Detectors/Modules under evaluation. The elements are mounted along $\simeq 1.4$ m of beam-line to within ± 0.5 mm in z-direction. The Sirocco strips are 30 μm wide providing a resolution of $\simeq 6\mu$m in x- and y-directions, while the Pixels are 50 μm $\times$ 400μ with a resolution on the order of 14μm $\times$ 115μm, depending on technology. The error matrices of the Sirocco points have in this context associated ellipsoids with aspect ratios of 83:1, the difference between fitting a 3D-line to these σ's and one to spherical σ's being 0.1 μm in the Telescope's mid-plane. The difference between χ^2_{exact} and χ^2_{approx} depends strongly on the impact angle of the track on the individual error ellipsoids:

$$\frac{\Delta\chi^2}{\chi^2_{exact}} = \frac{\left(\sigma_{xy}/\sigma_z\right)^2 + \left(\sigma_z/\sigma_{xy}\right)^2 - 2}{\left(n + 1/n\right)^2} \qquad (7)$$

For the Telescope setup this is 0.15 mrad, respectively $\Delta\chi^2$ on the order of 0.02%. However, for tracks impacting at 45^o, $\Delta\chi^2$ reaches towards 170ooo%, although $\Delta\sigma^2/\sigma^2_{exact} \simeq 1$.

For "stiff"-tracks, due to the constant impact angle on all points, $\Delta\chi^2 = const.$ along the trajectory, and the two methods yield identical results. If the track however, is measured piecewise in two different sub-systems, or it is composed of an ensemble of points with different σ's (different types of detectors), then even for straight tracks the two solutions differ.

For tracks bending in magnetic field the track's impact angle changes continuously along the track, $\Delta\chi^2$ following as:

$$d\left(\frac{\Delta\chi^2}{\chi^2_{exact}}\right) \Big/ \frac{\Delta\chi^2}{\chi^2_{exact}} = \frac{dn}{n} \cdot \frac{1-n^2}{1+n^2} \qquad (8)$$

Within the 1.4 m of the Telescope the 180 GeV/c particles bend in the B = 1.4 T magnetic field yielding a $\Delta\chi^2$ of 0.02% up front and 16% downstream, the approximative method pulling the fit increasingly tighter towards the end (0.5 μm per point), an effect evidently insignificant both in the Telescope setup as well as in the real B-physics context of ATLAS (p $\geq$ 1 GeV/c, B = 2.0 T, Δz $\simeq$ 0.14 m, respectively a point to point change of less than 4 % per %-$\Delta\chi^2$).

III. LINE FITS

Since in most cases it is possible to interchange the non-linear expression (3) with the quadratic expression (4), analytical solutions are available for two "stiff-track" situations. This either requires the particle to be out of magnetic field, or the field to be small with respect to the particle's momentum, incapable of bending its trajectory. It can also mean that the trajectory is measured only for a short distance, its deviation being insignificant with respect to the existing resolution.

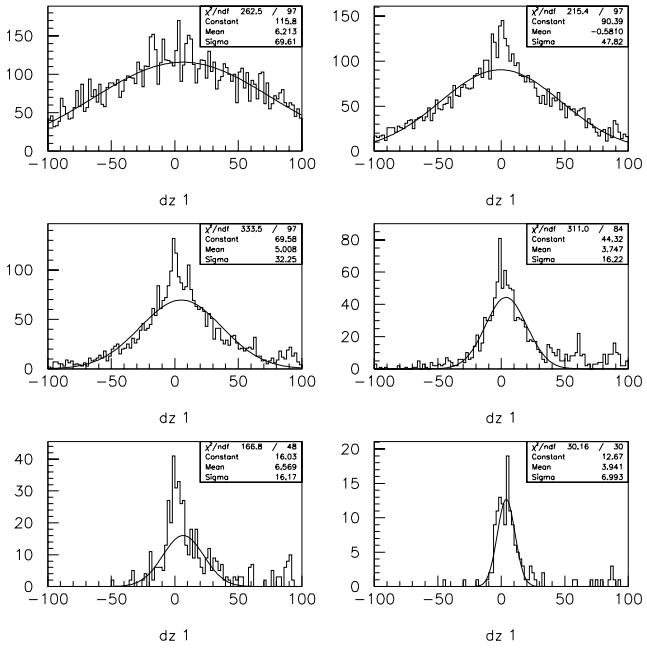

FIG. 1. Translational alignment parameter (Δz) histograms for N_{block} = 2, 4, 8, 20, 40 and 80 tracks. The effective number of track-fits in each histogram is $\simeq$ 3 million. In spite of the poor alignment lever arm for Δz (0.15 μm/mm at a σ = 6 μm detector resolution), the plots show strong improvement in Δz alignment-resolution with increasing N_{block}, electronics noise being cut-down by a factor of $1/\sqrt{N_{block}}$. The approach demands however extensive CPU power, analytical solutions being needed in order to keep the problem within capabilities of existing resources. All figures are in *mm*.

- The simplest fit is for $\sigma_j^2 = \sigma^2 \cdot \mathbf{1} = const.$:

$$\chi^2 = \sum_{j=1}^{N} \vec{\Delta_j}^{\,2} = min. \qquad (9)$$

Parametrising the tracks as:

$$\vec{r} = \vec{r}_0 + \lambda \vec{n} \qquad (10)$$

with $\vec{n}^2 = 1$ and $\vec{r}_0 \cdot \vec{n} = 0$, equation (9) becomes:

$$\chi^2 = \sum_{j=1}^{N} \vec{\delta_j}^{\,2} = min. \qquad (11)$$

where $\vec{\delta}_j = \vec{r}_j - \vec{r}_0 - \lambda_j \vec{n}$. The minimum condition implies locally $\lambda_j = \vec{r}_j \cdot \vec{n}$ and globally:

$$\vec{r}_0 = (\mathbf{1} - \vec{n}\vec{n}) \langle \vec{r} \rangle$$

$$\mathbf{M}\,\vec{n} = \mu_0\,\vec{n} \qquad (12)$$

with $\langle \vec{r} \rangle$ denoting average over the measured points, and $\mathbf{M} = \langle \vec{r}\,\vec{r} \rangle - \langle \vec{r} \rangle \langle \vec{r} \rangle$ the spread ellipsoid, around $\langle \vec{r} \rangle$. The 3 eigen-values of $\mathbf{M}$ represent the length of the track (μ_0), and the two transversal variances to the line-fit.

- For $\sigma_j^2 = diag(\sigma_x^2, \sigma_y^2, \sigma_z^2) = const.$ equation (11) holds again, however in normalised form, with $\sigma^{-1}\vec{r}_i$, $\sigma^{-1}\vec{r}_0$ and $\sigma^{-1}\vec{n}$. Adapted to the geometry of the Telescope Sirocco planes, this solution has been clocked to 0.033 μs/2D-fit and 2.6 μs/3D-fit[5] *vs.* 6100 μs/3D-fit for a MINUIT [2] driven routine. CPU-wise this permits the use of up to 2000 tracks per alignment block with a $\sqrt{N_{block}}$ proportional increase in alignment parameter resolution (figure 1), at a CPU cost proportional to N_{block}. **The 3600 times increase in speed yields a 60 fold increase in resolution over iterative routines, for the same amount of CPU time.**

  For a multi-tile pixel detector such as the ATLAS Inner Detector, this can mean the difference between affording a CPU-intensive high resolution alignment, or accepting a cut in the accessible physics[6]. Lack of CPU-power can rule out not only powerful physics methods, but also useful detector studies demanding the repeat of a procedure involving track-fits numerous times.

- An improvement to the Telescope 4-plane fit would be to consider the Pixel Demonstrators in the fit also. This would mean a fit to points with different error ellipsoids and the imposibility of "absorbing" all σ's into $\vec{r}_0$ and $\vec{n}$ in an unique way.

  For such $\sigma_i^2 \neq \sigma_j^2$ cases, the solution is given by a set of self-consistent equations:

$$\lambda_j = \frac{\vec{n} \cdot \sigma_j^{-2}(\vec{r}_j - \vec{r}_0)}{\vec{n} \cdot \sigma_j^{-2}\vec{n}}$$

$$\vec{r}_0 = \langle \vec{r} \rangle - \langle \lambda \rangle \vec{n}$$

$$\vec{n} = \frac{\langle \lambda \vec{r} \rangle - \langle \lambda \rangle \langle \vec{r} \rangle}{\langle \lambda^2 \rangle - \langle \lambda \rangle^2} \qquad (13)$$

  solvable in $\simeq 3$ iterations, starting from the previous analytical solution.

Having access to flash-routines, the Telescope alignment can be performed using a MINUIT driven parameter loop over blocks of 2000 tracks. The procedure yields very precise alignment parameters, the residuals for the Sirocco's being shown in figure 2 (top). The Pixel Detectors are aligned to first order analitically (exact solution), and tuned in a fashion similar to the Sirocco's for the rather low y-resolution effects on the x-resolution, and also for spurious χ^2 fits. The residuals for a set of two Pixel Detectors under test are shown in figure 2 (middle and bottom). The identical *side*-resolution of the pixels in x and y-directions (fit parameter P3) gives credit to the alignment that it yields physically tangible results (uniform technology on chip implies equal side-resolution in x and y).

IV. HELIX FITS

The helix fits for the Telescope test-stand in magnetic field must be performed in 3D due to the fringe field of the Spectrometer Magnet that bends the trajectory out of the xz-plane before the particle enters the magnet's active region. In addition, the incident particles impact the Telescope at $\simeq 0.15$ mrad to the normal, lying on the order of 100-200 μm out of the xz-plane.

[5] Both analytical solutions are 100% CPU-duty, *vs.* MINUIT at 70%, a remainder of 30% being idle CPU cycles.

[6] B-events can be selected with very high performance by applying a minimally missing $\vec{p}_\perp$ correction to the m_π evaluated vertex mass [3,4]. The method yields B-event samples with vertexing stand-alone purities on the order of 91-99% at corresponding efficiencies of 65-20%. This is of great impact for the B-Physics program at ATLAS and for searching the Higgs in the $H \to b\bar{b}$ channel ($80 < m_H < 110$ GeV/c^2). High purities ($c\bar{c} < 1\%$) at very competitive efficiency costs are possible only for such high-accuracy $\vec{p}_\perp$ corrections, respectively very good quality vertexing. In turn, vertexing performance is crucially dependent on alignment, needing flash reconstruction routines for precise, but CPU intensive methods.

A 3D-helix fit however is a relatively complicated procedure, the derivation of a semi-analytical algorithm being non-trivial.

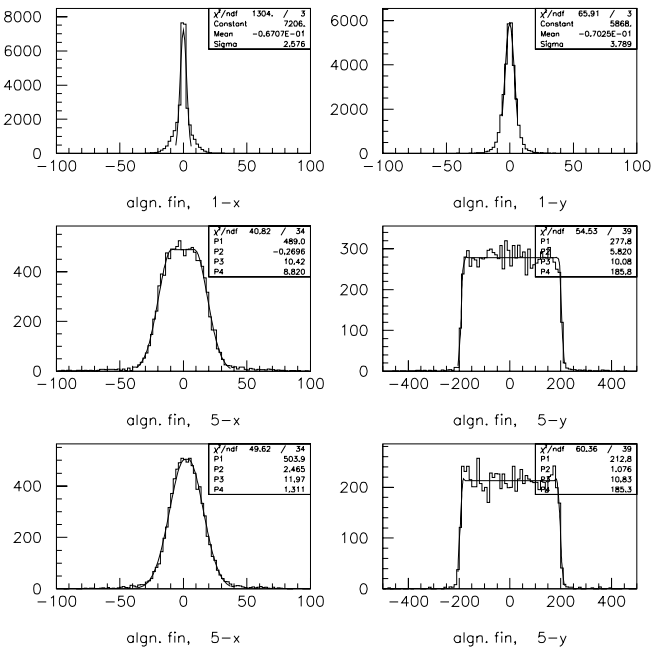

FIG. 2. Final alignment residuals for Sirocco plane-1 (top), $\sigma_x \simeq 3\ \mu$m, $\sigma_y \simeq 4\ \mu$m, and for two Pixel Detectors under test (middle and bottom). The equal *side*-resolution of the Pixels (parameter P3) in x and y-projection gives confidence that the alignment yields physically meaningful results. Parameter P4 gives the (single-hit) resolution of the pixel "hat". The center "thinning" of the Sirocco x-residuals (from a gaussian, by $\simeq 1$ μm) is supposed to be an effect of the residual magnetic field of the Spectrometer Magnet and of the Lorentz drift in the Sirocco strips. All figures are in μm.

On the other hand, iterative routines consum between 90000-300000μs/3D-fit, prohibiting the determination of a "weak" parameter - such as the radius of curvature, through a method as the one illustrated in figure 1. It is therefore worth investing the effort in constructing a semi-analytical flash-algorithm that can eliminate this obstacle.

In most of contemporary High Energy Physics experiments, and in particular in the Telescope set-up, helical tracks span less than 1^o of an arc (0.2^o in the case of the Telescope). It is therefore possible to do a 3D-helix fit semi-analitically, by curving perturbatively a line-fit to a helix.

In order to perform this operation, the target curve must be parametrised adequately, the best representation for a helix being derived from the solution to the particle in magnetic field, rather than from an abstract mathematical representation of the helix:

$$d_t\,\vec{p} = \frac{ec^2}{E}\,\vec{p}\times\vec{B}$$
$$d_t\,\vec{r} = \frac{c^2}{E}\,\vec{p} \qquad (14)$$

In the above, E is the particle's energy, $\vec{p}$ its momentum and $\vec{B}$ the magnetic field. The solution to equations (14) is:

$$\vec{r} = \vec{r}_0 + \lambda\vec{n} + \frac{\lambda^2}{2!}f\big(\frac{\lambda}{R}\big)\,\mathbf{F}\vec{n} + \frac{\lambda^3}{3!}g\big(\frac{\lambda}{R}\big)\,\mathbf{G}\vec{n} \qquad (15)$$

where $\lambda = \vec{v}_0 t = \omega R t$ is the linear distance travelled by the particle (or the *depth* of the helix), $\vec{\omega} = |e|c^2\vec{B}/E$ the helical rotation pulsation, $\vec{n} = \vec{p}_0/p_0$ the direction of *engagement* of the particle on the magnetic field region, $R = p_0/|e|B$ a parameter related to the radius of curvature of the helix $R_{helix} = R\sqrt{1-(\vec{n}\cdot\vec{n}_B)^2}$, $\vec{n}_B = e\vec{B}/|e|B$, and $f(\zeta)$ and $g(\zeta)$ two functions:

$$f(\zeta) = \frac{2!}{\zeta^2}(1 - cos\zeta) \simeq 1$$
$$g(\zeta) = \frac{3!}{\zeta^3}(\zeta - sin\zeta) \simeq 1 \qquad (16)$$

that for $\zeta \to 0$ approximate to unity, respectively $\mathbf{F}$ and $\mathbf{G}$ two tensors:

$$\mathbf{F} = \times\,\vec{C}$$
$$\mathbf{G} = \vec{C}\,\vec{C} - \vec{C}^2\cdot\mathbf{1} \qquad (17)$$

satisfying $\mathbf{F}^\dagger = -\mathbf{F}$, $\mathbf{G}^\dagger = \mathbf{G}$, $\mathbf{FG} = \mathbf{GF} = \vec{C}^2\mathbf{F}$, $\mathbf{F}^2 = \mathbf{G}$, and $\mathbf{G}^2 = -\vec{C}^2\mathbf{G}$. The vector $\vec{C}$ is $\vec{C} = \vec{n}_B/R$.

It is evident that for $R \to \infty$, or equivalently $\lambda \to 0$, expression (15) reduces to the parametrisation of the line (10) used in performing line fits. The second and third order terms in λ perturb the line to a helix, and in most of current HEP experiments $f(\zeta) \simeq 1$ and $g(\zeta) \simeq 1$. The limiting factors for this approximation are:

- **geometric** - the arc of helix should not have a *depth* beyond the approximation validity for $f(\zeta)$ and $g(\zeta)$. This is related to the demanded resolution σ and the particle's momentum:

$$p \geq \frac{\lambda}{16(\sigma/\lambda)^{1/3}} \simeq 5\ GeV/c \tag{18}$$

where in the above, λ and σ are expressed in [m] and p in [GeV/c]. The value for the minimum momentum is for the Telescope setup.

- **dE/dx** - the loss of energy along the trajectory determines a "tighter" helix. Over a small arc, or for high momentum, this is negligible. With respect to the existing resolution, the momentum should satisfy:

$$p \geq \frac{0.3B\sigma}{\lambda} \simeq 0.004\ GeV/c \tag{19}$$

where in the above the helix *depth* λ is expressed in radiation lengths, σ in [m] and p in [GeV/c]. The value for the minimum momentum is for the Telescope setup.

- **multiple scattering** - the deviation from the direction of flight of the particle can be significant, the necessary momentum for obtaining a resolution σ being:

$$p \geq 0.006 \left(\frac{\lambda}{\sigma}\right)\sqrt{\lambda} \simeq 340\ GeV/c \tag{20}$$

where in the above, λ and σ are expressed in radiation lengths and p in [GeV/c]. It should be noted however that in the case of the Telescope this is the single plane resolution, and not that of the test-stand together, which requires p $\geq$ 180 GeV/c for a resolution of 3-4 μm. The value for the minimum momentum is for the Telescope setup.

The semi-analitical helix fit procedure has 3 steps:

1. Estimation of $\vec{n}$, the engagement direction of the particle on the magnetic field. This is obtained with small CPU demand by a 3D line flash-fit to the first 3-4 points of the trajectory. The vector $\vec{n}$ is eigen-vector of $\mathbf{M} = \langle \vec{r}\vec{r} \rangle - \langle \vec{r} \rangle \langle \vec{r} \rangle$, hence any perturbation $\mathbf{M}_{helix} = \mathbf{M}_{line} + \delta\mathbf{M}$ changes it only to second order.

2. Using $\vec{n}$ found above, the second order term corrections to $\vec{r}_0$ and λ_i can be estimated:

$$\begin{aligned} \Delta\lambda_i &= \frac{\lambda_i}{R}(\vec{r}_i - \vec{r}_0) \cdot \vec{n} \times \vec{n}_B \\ \Delta\vec{r}_0 &= \langle \vec{r} \rangle - \vec{r}_0 - \langle \lambda \rangle \vec{n} - \frac{\langle \lambda^2 \rangle}{2R} \vec{n} \times \vec{n}_B \end{aligned} \tag{21}$$

computations again only modestly CPU demanding.

3. Introducing the third order term and using the previously corrected $(\vec{n}, \vec{r}_0, \lambda_i)$, local and global equations for the parameters can be written:

$$\begin{aligned} &(\vec{n} + \lambda_i \mathbf{F}\vec{n} + \frac{\lambda_i^2}{2}\mathbf{G}\vec{n}) \cdot \vec{\rho}_i = 0 \\ &\langle\, (\lambda \cdot \mathbf{1} - \frac{\lambda^2}{2}\mathbf{F} + \frac{\lambda^3}{6}\mathbf{G})\vec{\rho}\, \rangle = 0 \\ &\langle\, \vec{\rho}\, \rangle = 0 \end{aligned} \tag{22}$$

where $\vec{\rho}_i$ are the residuals of the points to the fitted curve:

$$\vec{\rho}_i = -\vec{r}_i + \vec{r}_0 + \lambda_i \vec{n} + \frac{\lambda_i^2}{2}\mathbf{F}\vec{n} + \frac{\lambda_i^3}{6}\mathbf{G}\vec{n} \tag{23}$$

Expanding to first order, the coresponding corrections $(\Delta\vec{n}, \Delta\vec{r}_0, \Delta\lambda_i)$ must satisfy:

$$\begin{aligned} &\alpha_i \Delta\lambda_i + \vec{a}_i \Delta\vec{n} + \vec{b}_i \Delta\vec{r}_0 + \beta_i = 0 \\ &\langle \vec{a}\, \Delta\lambda \rangle + \langle \lambda^2 \rangle \cdot \mathbf{1}\Delta\vec{n} + \mathbf{D}\Delta\vec{r}_0 + \vec{\delta} = 0 \\ &\langle \vec{b}\, \Delta\lambda \rangle + \mathbf{D}^\dagger \Delta\vec{n} + \mathbf{1} \cdot \Delta\vec{r}_0 + \vec{\sigma} = 0 \end{aligned} \tag{24}$$

where:

$$\begin{aligned} \alpha_i &= \vec{n}\vec{n} - \vec{r}_i\mathbf{F}\vec{n} + \vec{r}_0\mathbf{F}\vec{n} \\ \beta_i &= \vec{r}_0\vec{n} - \vec{r}_i\vec{n} + \lambda_i\vec{n}\vec{n} + \lambda_i\vec{r}_0\mathbf{F}\vec{n} - \lambda_i\vec{r}_i\mathbf{F}\vec{n} + \\ &\quad \frac{1}{2}\lambda_i^2\vec{r}_0\mathbf{G}\vec{n} - \frac{1}{2}\lambda_i^2\vec{r}_i\mathbf{G}\vec{n} + \frac{1}{6}\lambda_i^3\vec{n}\mathbf{G}\vec{n} \\ \vec{a}_i &= \vec{r}_0 - \vec{r}_i + 2\lambda_i\vec{n} + \lambda_i\mathbf{F}\vec{r}_i - \lambda_i\mathbf{F}\vec{r}_0 \\ \vec{b}_i &= \vec{n} + \lambda_i\mathbf{F}\vec{n} \\ \vec{\delta} &= \langle\lambda\rangle\vec{r}_0 - \langle\lambda\vec{r}\rangle + \langle\lambda^2\rangle\vec{n} + \frac{1}{2}\mathbf{F}\langle\lambda^2\vec{r}\rangle - \\ &\quad \frac{1}{2}\langle\lambda^2\rangle\mathbf{F}\vec{r}_0 + \frac{1}{6}\langle\lambda^3\rangle\mathbf{G}\vec{r}_0 - \frac{1}{6}\mathbf{G}\langle\lambda^3\vec{r}\rangle + \\ &\quad \frac{1}{12}\langle\lambda^4\rangle\mathbf{G}\vec{n} \\ \vec{\sigma} &= \vec{r}_0 - \langle\vec{r}\rangle + \langle\lambda\rangle\vec{n} + \frac{1}{2}\langle\lambda^2\rangle\mathbf{F}\vec{n} + \frac{1}{6}\langle\lambda^3\rangle\mathbf{G}\vec{n} \\ \mathbf{D} &= \langle\lambda\rangle \cdot \mathbf{1} - \frac{1}{2}\langle\lambda^2\rangle\mathbf{F} \end{aligned} \tag{25}$$

By eliminating $\Delta\lambda_i = -(\beta_i + \vec{a}_i\Delta\vec{n} + \vec{b}_i\Delta\vec{r}_0)/\alpha_i$ equations (24) become:

$$\begin{aligned} \mathbf{M}\Delta\vec{n} + \mathbf{N}\Delta\vec{r}_0 &= \vec{\tau} \\ \mathbf{N}^\dagger\Delta\vec{n} + \mathbf{R}\Delta\vec{r}_0 &= \vec{\pi} \end{aligned} \tag{26}$$

where:

$$\mathbf{M} = \langle \frac{\vec{a}\,\vec{a}}{\alpha} \rangle - \langle \lambda^2 \rangle \cdot \mathbf{1}$$

$$\mathbf{N} = \langle \frac{\vec{a}\,\vec{b}}{\alpha} \rangle - \langle \lambda \rangle \cdot \mathbf{1} + \frac{1}{2}\langle \lambda^2 \rangle \mathbf{F}$$

$$\mathbf{R} = \langle \frac{\vec{b}\,\vec{b}}{\alpha} \rangle - \mathbf{1} \qquad (27)$$

and :

$$\vec{\tau} = \vec{\delta} - \langle \frac{\beta\,\vec{a}}{\alpha} \rangle$$

$$\vec{\pi} = \vec{\sigma} - \langle \frac{\beta\,\vec{b}}{\alpha} \rangle \qquad (28)$$

To zeroth order all three $\mathbf{M}$, $\mathbf{N}$ and $\mathbf{R}$ are proportional to $(\mathbf{1} - \vec{n}\vec{n})$, the non-invertable perpendicular projection on $\vec{n}$, by factors of $\langle \lambda^2 \rangle$, $\langle \lambda \rangle$ and 1.

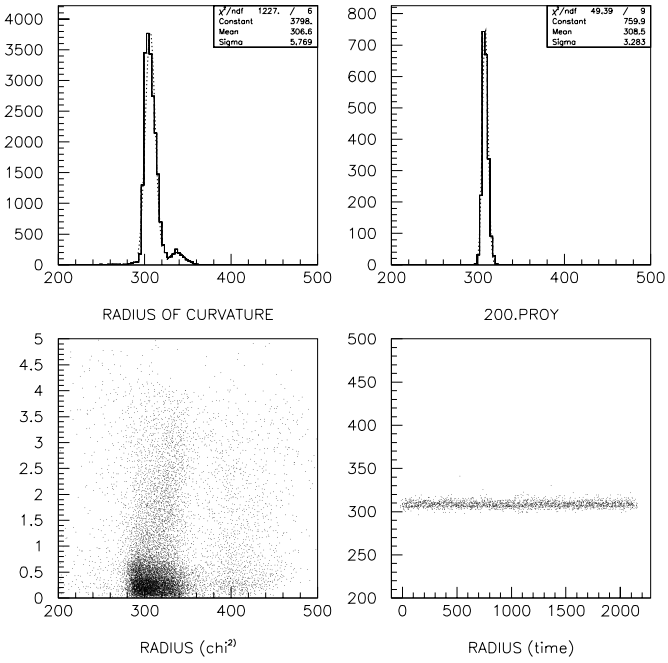

FIG. 3. Normal-impact equivalent radius of curvature for single tracks (top-left) and coresponding χ^2 of fit *vs.* radius of curvature (bottom left). Resolution is $\simeq$ 6m for an average radius of curvature of 307m. Using blocks of 10 tracks (top-right) the resolution improves to $\simeq$ 3.3m, the stability of the SPS delivered beam being tracked *vs.* time bottom-right.

Therefore in the numerical approach the inversion is obtained by decomposing the operators into a part proportional to $(\mathbf{1} - \vec{n}\vec{n})$ and a "remainder":

$$\mathbf{R} = (\mathbf{1} - \vec{n}\vec{n}) \cdot (2tr\mathbf{R} - \mathbf{R}_{\vec{n}\,\vec{n}} - \mathbf{R}^{\dagger}_{\vec{n}\,\vec{n}})/4 + ... \quad (29)$$

The solution $(\Delta\vec{n}, \Delta\vec{r}_0, \Delta\lambda_i)$ is thus:

$$\Delta\vec{n} = (\mathbf{R}\mathbf{N}^{-1}\mathbf{M} - \mathbf{N}^{\dagger})^{-1}(\mathbf{R}\mathbf{N}^{-1}\vec{\tau} - \vec{\pi})$$

$$\Delta\vec{r}_0 = \mathbf{N}^{-1}(\vec{\tau} - \mathbf{M}\Delta\vec{n})$$

$$\Delta\lambda_i = -\frac{1}{\alpha_i}(\beta_i + \vec{a}_i\vec{n} + \vec{b}_i\Delta\vec{r}_0) \qquad (30)$$

For notation purposes although not mentioned, all quantities used are considered normalised - *i.e.* $\sigma^{-1}\vec{r} \to \vec{r}$.

The CPU demand of the 3 steps is under 15 μs. For better precision however, the last step can be repeated twice, bringing the 3D-helix fit to 22 μs, respectively **at least 4000 times faster** than any iterative version of the fit.

Using the fit on blocks of 2000 tracks the alignment in magnetic field is checked and adjusted. The fit is then used with blocks of 10 tracks for a fine scan of the energy of the beam delivered by the SPS. This is expressed in normal-impact radius of curvature equivalent and is shown in figure 3 (bottom-right).

V. CONCLUSIONS

Analytical methods are shown to have a dramatic impact on line and helix fits, bringing down CPU usage by 3-4 orders of magnitude. The fit methods developed have been used with succes in the alignment and data reconstruction of the ATLAS Pixel Detector test-beam stand, and can be of significant use for the precise alignment and reconstruction in the real ATLAS B-physics context. Access to very high accuracy vertexing, dependent on precise alignment, enables the dramatic increase in purity of B-event selection, by applying a $\vec{p}_{\perp}$ correction to the m_{π} evaluated B-vertex mass.

I am thankful to the High Energy Physics group of Wuppertal University for its hospitality and the facilities provided during completion of this work under an Alexander von Humboldt Foundation grant, and to the ATLAS Pixel Detector Collaboration for the opportunity of engaging in this interesting research.

[1] M. Dima, *SLAC-R-0505*, SLAC Report, p. 100, SLAC 1997
[2] MINUIT v94.1 minimization program, F. James, F. Roos, CERN (1967).
[3] ALEPH Collaboration, *CERN-PPE/97-017*, CERN 1997
[4] SLD Collaboration, *SLAC-PUB-7481*, SLAC 1997